CrossMark

RESEARCH ARTICLE

Alternative Reducing Agents in Metallurgical Processes: Gasification of Shredder Residue Material

Samira Lotfian[1] · Hesham Ahmed[1,2] · Abdel-Hady A. El-Geassy[2] · Caisa Samuelsson[1]

Abstract Shredder residue material (SRM) contains plastic material, which has a potential to replace metallurgical coal for reduction during bath-smelting processes. Among the important parameters affecting its implementation are the gasification and the reactivity of char. Therefore, prior to considering its application in metallurgical processes, the gasification characteristics of the produced char need to be studied. Although the char produced from SRM contains lower fixed carbon compared with coal char, it has a porous structure and high surface area, which makes it highly reactive during gasification experiments. In addition to physiochemical properties, the catalytic effect of ash content of SRM char is attributed to its higher reactivity and lower activation energy compared with coal char. Furthermore, the effect of devolatilization heating rate on the gasification characteristics of produced char is investigated. It was found that the devolatilization heating rate during char production has a considerable effect on morphological properties of the char product. Moreover, the gasification reactivity of char produced at a fast devolatilization heating rate was the highest, due to the less crystalline structure of the produced char.

List of Symbols

X	Char conversion
w_0	Initial weight of char
w_∞	Saturation value of the weight-loss curve
$w(t)$	Sample weight at a time t
r	Gasification rate of the isothermal gasification
ρ	Gasification rate of the nonisothermal gasification
E_a	Activation energy
A	Preexponential factor
R_S	Reactivity index
τ_{50}	Time (in minute) required to reach the carbon conversion of 50 %
w_C	Weight of carbon in the sample remaining unreacted at the time t

✉ Samira Lotfian
   samira.lotfian@ltu.se

   Hesham Ahmed
   hesham.ahmed@ltu.se

   Abdel-Hady A. El-Geassy
   caisa.samuelsson@ltu.se

   Caisa Samuelsson
   elgeassy@yahoo.com

[1] MiMer, Luleå University of Technology, 97187 Luleå, Sweden

[2] Department of Minerals Technology and Processing, Central Metallurgical Research and Development Institute (CMRDI), P.O. Box 87, Helwan, Cairo, Egypt

Introduction

Shredder residue material (SRM) is the residue from shredding of end-of-life equipment, after removal of the main metallic content. SRM is an inhomogeneous material consisting of metals and ceramics, in addition to organic materials such as different types of plastics [1]. The amount of SRM is ever increasing, and the material is currently mainly landfilled or incinerated. The proper management of this complex residue material is a growing concern. Although SRM does not contain enough metals to

be economically feasible as a secondary raw material in metallurgical processes, it contains considerable quantities of plastic materials. Plastic materials contain carbon and hydrogen, which makes them a possible alternative reducing agent [2]. Injection of plastic material in blast furnace has been reported in the literature and implemented in several industrial plants [2–4]. One limitation in using plastic-containing residue material for iron making is the content of metals such as zinc and copper which are not desirable in iron-making processes [5]. Therefore, utilizing plastic-containing residue material in nonferrous processes is more feasible and has no detrimental effect on final product quality. Therefore, SRM has the potential to replace part of the fossil coal used for reduction of oxides in bath-smelting processes.

Thermal decomposition of coal and its interaction with the melt in bath-smelting processes are studied [6]. In these processes, pulverized coal is injected alongside air into molten slag. The coal particles that are entrained in the melt release moisture and devolatilize instantaneously, forming a gaseous envelop, which surrounds the remaining char [7]. At the interface of the gaseous envelop with the molten slag, oxides are reduced by CO and H_2 [8]. The CO_2 produced from the reduction reaction diffuses inside the bubble and reacts with carbon in char, generating CO via the Boudouard reaction with carbon in char, as illustrated in Fig. 1. The hydrogen content of volatiles also participates in the reduction through an equivalent reaction to produce H_2O [7]. Carbon in char can react with CO_2, H_2O, or O_2, where reaction of O_2 is very fast and reaction with H_2O is insignificant. Therefore, the rate of CO_2 gasification of chars is the lowest and the most significant, and consequently, it is considered as the rate-determining step during thermal decomposition [9].

Gasification of plastic materials has been reported in the literature [10, 11]; however, in these studies, the material is heated up under CO_2 atmosphere. In this way, simultaneous devolatilization and gasification as well as volatile interaction with CO_2 will occur. Consequently, char gasification characteristics are very difficult to determine. Since in metallurgical applications, the reducing agent could participate in reactions through volatiles or fixed carbon in char, it is important to study these two stages separately. In addition, in the literature, there is a lack of study of a complex material such as SRM, which is a mixture of plastics alongside inorganic materials. Most studies deal with the gasification of char produced from individual plastics [9, 12, 13]. As an example, Wu et al. [9] studied the effect of physiochemical properties and gasification temperature on the conversion rate of char derived from three common plastics in electronic scrap at 873 K. Results showed that as the gasification temperature increases, the conversion time decreases, and the

gasification reactivity was the highest for char with the highest surface area and the lowest carbon crystalline degree.

In the present investigation, the aim is to study and compare the gasification of SRM as an alternative reducing agent with the current reducing agent, coal. Gasification reaction and char reactivity are influenced not only by the nature of material but also by the conditions during the devolatilization stage. One of the devolatilization parameters is the heating rate, which greatly differs between lab scale and real operation conditions. Therefore, the effect of devolatilization heating rate on the produced char is studied.

Materials and Methods

SRM and coal samples as reference material for comparison purposes were used to produce char samples. Ultimate analysis based on standard[1] was carried out for all samples by the certified laboratory ALS Scandinavia AB, Sweden. Proximate analyses of original samples and char samples were performed using thermogravimetric analyzer (TGA, Netzsch Thermal Analyzer STA 409); the results are presented in Table 1. Proximate analysis involves heating the sample in Argon (99.999 % purity) at a heating rate of 10 K/min from room temperature to 383 K with a holding time of 10 min to remove moisture. In the next step, the samples were heated up to 1223 K. The weight loss in this stage is associated with the volatile content. After the sample reached a constant weight loss (i.e., devolatilization is completed), argon was replaced by air to oxidize the residual char; the observed weight loss corresponds to the fixed carbon content. During this stage, the metals in SRM can also be oxidized affecting weight change. The remaining residue represents the ash content of the material [14].

Char Preparation

Pulverized coal with particle size of less than 38 μm (as received) and SRM with particle size of less than 0.5 mm, with average weight of 5 g were devolatilized in a vertical tube furnace. A schematic representation of the furnace is shown in Fig. 2. The furnace consisted of a kanthal wire-wound tube furnace (length: 100 cm, diameter: 12.5 cm). A stainless steel tube (length: 135 cm, outer diameter: 6.5 cm) closed at the bottom end was placed inside the
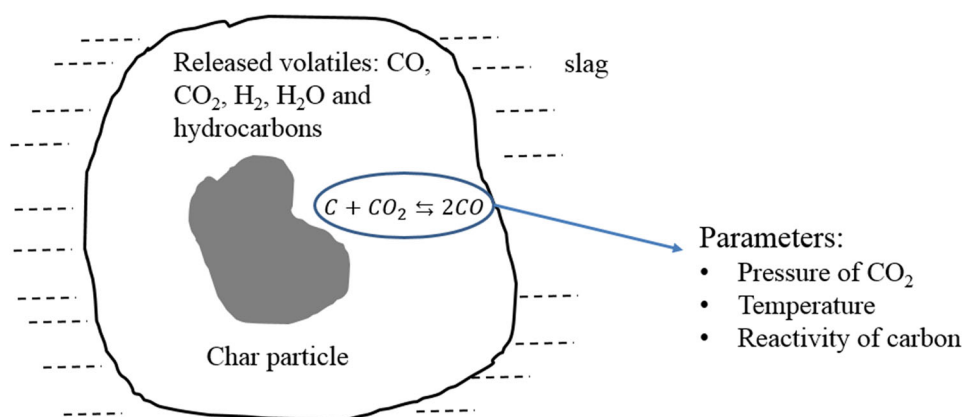
Table 1 Ultimate and proximate analyses of original SRM and coal samples

	H (wt%)	O (wt%)	N (wt%)	S (wt%)	C (wt%)
Ultimate analysis by standard					
Coal	4.8	5.2	1.3	0.3	84.0
Shredder residue material	6.1	12.0	1.8	0.08	56.9
	Moisture (wt%)	Volatile (wt%)	Fixed carbon (wt%)	Ash (wt%)	
Proximate analysis by thermogravimetric analyzer					
Coal	0.4 ± 0.3	22.7 ± 0.4	66.7 ± 1.6	9.2 ± 2.4	
Shredder residue material	0.6 ± 0.3	66.9 ± 5.2	9.3 ± 1.9	23.2 ± 6.3	

furnace. Nitrogen (99.996 % purity) at flow rate of 10 l/min enters from the bottom passing through alumina beads to be heated up before it reaches the evenly heated zone. Nitrogen and volatiles released leave the furnace from the outlet at the top. Weight loss was continuously monitored with a balance at the top of the furnace. A K-type thermocouple is positioned at the evenly heated zone of the furnace to measure the furnace temperature. The sample is introduced close to the thermocouple, in the alumina crucible.

Char Samples Produced at Slow and Medium Devolatilization Heating Rates

The sample was placed in an alumina crucible (height of 63 mm and thickness of 0.7 mm) and introduced to the furnace, suspended from the balance. Initially, N_2 was introduced to the furnace for 15 min to ensure inert atmosphere, then the sample was heated up to 1173 K at a heating rate of 2 K/min (slow devolatilization). Another sample was heated up at an average heating rate of 8 K/min (medium devolatilization). Once the sample reached the desired temperature, it was removed from the heated zone and placed in the water cooled zone, where the char sample was cooled to room temperature in N_2 atmosphere.

Char Samples Produced at Fast Devolatilization Heating Rate

The furnace was heated to 1173 K, and N_2 at a flow rate of 10 l/min was introduced and maintained for 15 min. The sample placed in the alumina crucible was then introduced to the heated zone of the furnace and held until the weight loss stabilized. To estimate the heating rate during fast devolatilization and ensure a uniform heating of the sample, two thermocouples were inserted: one inside the sample, and one next to the alumina crucible, and it was shown that the temperature rose to 1173 K in 5 min, i.e., the average heating rate is 180 K/min. The temperature drop in the water-cooled zone was also monitored using the thermocouple inside the sample. It showed that the temperature decreased from 1173 K to about 333 K, in 10 min. This cooling rate is valid during slow and medium devolatilizations as well. The heating cycles for all three char samples are presented in Fig. 3.

Char Characterization

Proximate analysis of char samples was determined using thermogravimetric analyzer, with the same procedure as for the original samples. Porosity and pore size distribution of
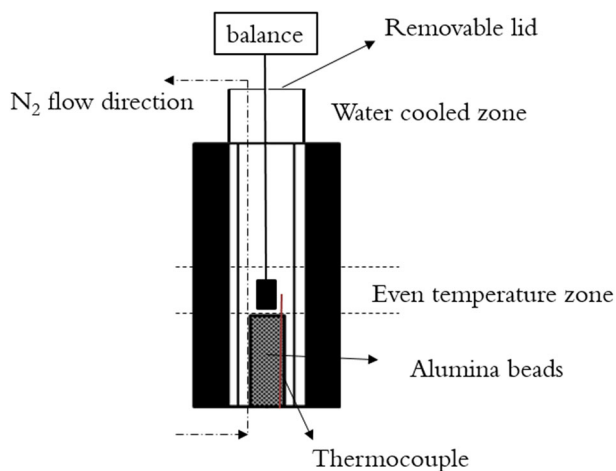
Fig. 2 Schematic of tube furnace

char samples were measured using a mercury porosimeter (Pore sizer 9320, micrometrics, USA). Mercury porosimetry is based on the gradual injection of liquid mercury into an evacuated pore at different applied pressures [15]. The surface area of char samples was measured using Micromeritics' flowsorb II 2300 and calculated by applying the Brunauer–Emmett–Teller (BET) equation to the adsorption/desorption isotherm (N_2–He, 77 K). Morphology of produced char samples was studied using Zeiss Gemin Merlin scanning electron microscopy (SEM). A PANalytical Empyrean X-ray diffractometer equipped with copper K_α radiation was used to record the X-ray diffraction spectra of SRM char samples. The chemical analysis

of SRM ash was performed in Boliden's-Rönnskär laboratory. Cr, Al, and Mg contents of SRM ash were determined by atomic absorption spectroscopy (AAS), where the samples were prepared by dissolving in Na_2O_2. The other elements were measured by dissolving in HCl and HNO_3 and analyzed using inductively coupled plasma (ICP). The chemical analysis of coal ash was measured by the certified laboratory ALS Scandinavia AB, Sweden. The sample was fussed with $LiBO_2$ and dissolved in HNO_3. Finally, the elements were measured by ICP.

Gasification Experiment

Initial gasification experiments were performed isothermally using TGA. Char samples were manually crushed and sieved to a particle size of less than 100 μm. For this particle size range, it has been reported that the chemical reaction controls the kinetic of reaction and the effect of reactant diffusion is negligible [16]. In order to further minimize the interference of mass and heat transfer on gasification reaction, an initial set of experiments was performed. The conditions were selected to ensure the easy escape of locally produced CO and easy access of CO_2 to the reaction sites. Based on these experiments, sample weights of 10 mg and 20 mg were selected for coal and SRM char, respectively. The char samples produced at medium devolatilization heating rate were heated up to different temperatures 1073–1473 K with an interval of 50 K, under Argon (99.999 % purity) atmosphere at heating rate of 10 °C/min. Once the

Fig. 3 Heating cycles of char samples produced at slow, medium, and fast heating rates
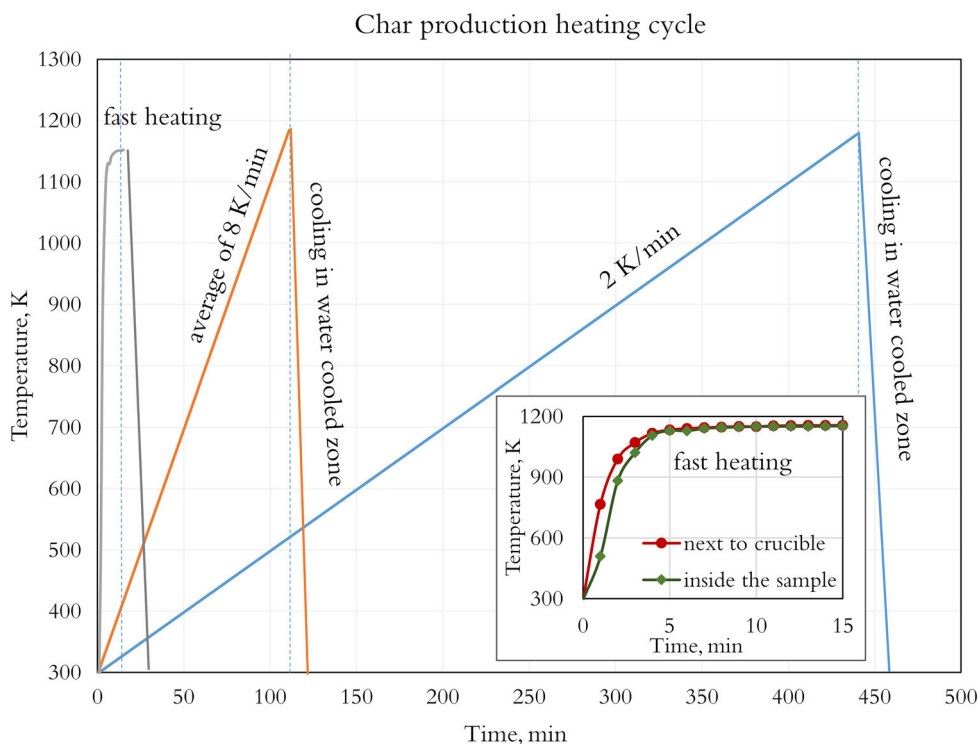
sample temperature stabilized at the desired temperature, the atmosphere was switched to CO_2 (99.998 % purity) at a flow of 200 ml/min and maintained for one hour. The char conversion is computed as a function of time [17]:

$$X = \frac{w_0 - w(t)}{w_0 - w_\infty} \tag{1}$$

Gasification rate is defined as differential of carbon conversion to gasification time:

$$r = -\frac{1}{w_0 - w_\infty} \frac{dw}{dt} = \frac{dX}{dt} \tag{2}$$

Gasification of char is a heterogeneous gas–solid reaction; as CO_2 is in excess, its partial pressure remains constant during the reaction. Therefore, the reaction rate constant is dependent on temperature and the kinetic parameters such as activation energy and preexponential factor can be calculated using the Arrhenius equation [18]:

$$r = Ae^{-E_a/(RT)} \tag{3}$$

In general, to evaluate the overall gasification reactivity of char, reactivity index is used, which is defined by Eq. 4 [19]:

$$R_S = \frac{0.5}{\tau_{50}} \tag{4}$$

Furthermore, to study the effect of devolatilization heating rate on gasification of char samples, the slow and fast devolatilized char were tested under nonisothermal condition, which has the advantage of studying the reaction in one experiment [20]. The kinetic parameters were calculated based on the assumption that the nonisothermal heating cycle consists of an infinite number of discrete isothermal sections, which are a first order reaction. The previously mentioned Arrhenius equation can be applied to those isothermal sections, with the modification of considering the weight of remaining carbon in the sample for each isothermal section [21]. 10 mg of char samples were heated up to 623 K under argon at a flow rate of 100 ml/min at a heating rate of 20 K/min. Afterward, the heating rate was changed to 2 K/min, while CO_2 at a flow of 200 ml/min was introduced. The samples were heated up to 1173 K. The kinetic parameters are calculated based on Eq. 5.

$$\rho = \frac{1}{w_C} \frac{dw_C}{dt} = Ae^{-E/RT} \tag{5}$$

Results and Discussion

Characterization of Char Samples

Proximate Analysis

The proximate analyses of char samples produced at different devolatilization heating rates are presented in

Table 2. Comparison of the proximate analyses of coal and SRM char shows that SRM contains lower fixed carbon compared to that of coal. Coal char contain up to 80 % fixed carbon, while SRM char has 20 % fixed carbon. The proximate analyses of both SRM and coal char samples do not significantly change at different devolatilization rates.

Higher amounts of volatiles are present in SRM char compared with coal char. Mass spectroscopy analysis during proximate analysis of char shows the evolution of H_2 and H_2O, which implies incomplete reactions during char production. It is known that, at the final stage of devolatilization, H_2 is produced by the recombination of aromatic compounds [22]. Release of H_2 during proximate analysis of char suggests the continuation of these reactions. H_2O is probably produced from reduction reaction of oxides in ash with produced hydrogen. Finally, SRM has higher content of ash compared with coal, due to its content of metals and ceramic materials. A summary of elemental analysis of ash for coal and SRM is presented in Tables 3 and 4.

SRM char contains a lower amount of fixed carbon than coal char, which is due to the fact that SRM consists of plastics, which are known to produce lower amounts of fixed carbon compared with coal. Crosslinking and cyclization reactions are the important reactions that determine the amount of char produced during plastic thermal decomposition. Thus, some plastics such as polyethylene are decomposed mainly by release of volatiles (98 %), generating a low amount of char, while a plastic like polyvinylchloride produce a higher amount of char [23].

Pore Size Distribution and Surface Area of Char Samples

The characteristics of char samples prepared at slow and medium heating rates are similar; therefore the characterization results from the slow devolatilized char are presented and compared with the fast devolatilized char. Figure 4a shows the variation between cumulative intrusion measurements of the intruded Hg in coal and coal char samples versus the corresponding pore diameter. Cumulative intrusion volume is a plot of the volume of mercury intruded into each gram of samples as a function of pore diameter [24].

Figure 4 shows that the cumulative intrusion in original the coal sample differs from the char samples produced at slow and fast devolatilization heating rates. In the original sample, the total intrusion volume of Hg gradually increases for a pore size range of 5–200 μm, then sharply increases at pore diameters in the range of 0.3–3 μm, followed by a gradual increase. The cumulative intrusion volume observed for both the treated char samples were higher than the original coal sample in the pore size range

Table 2 Proximate analyses of coal and SRM char

	Heating rate (K/min)	Moisture (%)	Volatile (%)	Fixed carbon (%)	Ash (%)
Coal char	Slow	0.5	2.5	83.1	13.9
	Medium	0.6	2.7	84.8	12.1
	Fast	0.8	1.6	84.3	13.3
SRM char	Slow	1.6	10.2	23.6	64.0
	Medium	1.8	9.0	23.2	66.0
	Fast	2.3	9.4	23.1	65.2

Table 3 The elemental composition of SRM ash

Element in ash	Ca	Si	Cu	Al	Mg	Ti	Cr	Fe	Zn	Na
Wt%	12.9	12.6	11.5	11.0	2.6	2.3	0.6	0.4	0.3	0.1
Other elements detected in ash in ppm level	Pb, Mo, Se, V, Co, Cd, As, Be, Sb, Ni, Mn									

Table 4 The elemental composition of coal ash

Elements in ash	Si	Al	Ca	Fe	Mg
Wt%	0.5	0.2	0.5	0.5	0.2
Other elements detected in ash in ppm level	K, Na, P, Mn, Ti, Ba, be, Cr, Nb, W, Sc, Sr, Zr				

of 5–200 μm, while in the pore diameters in the range of 0.3–3 μm, the original sample was higher than that in the coal char samples. The latter pore size range almost disappeared for char samples. The population of pore size in the size range of 5–200 μm increased in the order of, fast devolatilized char > slow devolatilized char > original sample. This indicates that at the higher devolatilization heating rate, a larger number of macropores is formed at the expense of smaller pores.

Figure 4b shows the variation between the cumulative intrusion of Hg versus the pore diameter in the original SRM and the SRM char samples. There is a gradual increase in the total intruded volume of Hg for the pore size range of 5–200 μm for all samples; afterward, the slopes decrease slightly. The original sample shows an increase in the cumulative pore volume for the 0.03–0.001 μm, indicating the presence of micropores, which disappear in the char samples. The cumulative intrusion volume decreases with the increase in the devolatilization heating rate as compared with the original SRM sample. This indicates that, unlike the coal sample, at a slow devolatilization rate a larger number of pores are formed.

The effect of heating rate during the devolatilization step on the surface area of the corresponding produced coal and SRM char samples is shown in Table 5. For both SRM and coal char samples, the surface area is not significantly affected by the devolatilization heating rate; however, char samples produced at fast heating show a slight increase in surface area, compared to that produced at a slow
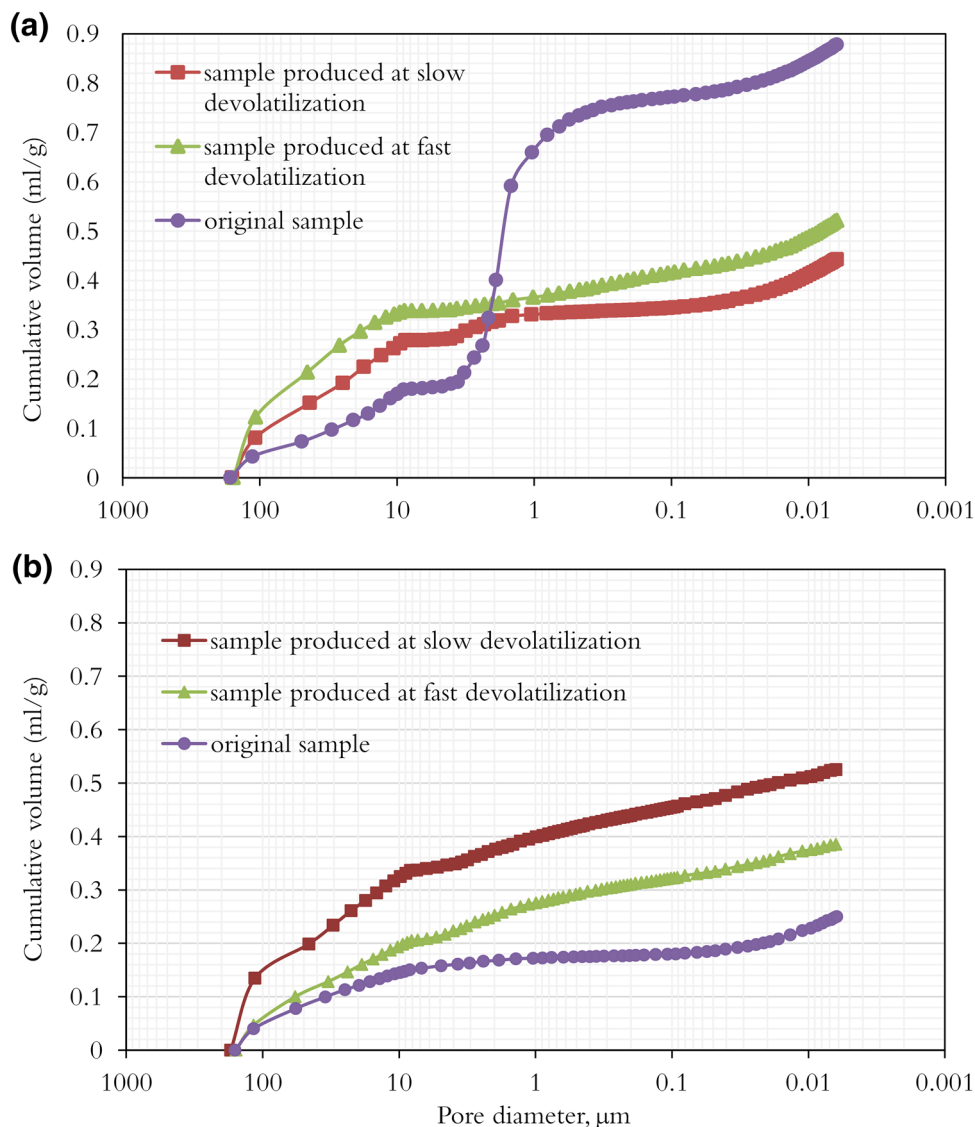
devolatilization heating rate. This could be due to the slight sintering at slow and medium devolatilization. At any devolatilization heating rate, the surface area of the produced SRM char samples is higher than that of coal chars.

Morphology of Char Samples

The morphology of the char samples produced at fast and slow devolatilization heating rates was studied using scanning electron microscopy (SEM). Coal char produced by fast devolatilization (Fig. 5) shows a more porous structure compared with char produced at a slow heating rate. This is in agreement with the result of mercury porosimetry indicating higher population of macropores observed in char produced at a fast heating (Fig. 4a). A closer examination of the morphology shows that char produced at a slow devolatilization rate consists of individual particles in the size range of the original coal sample (Fig. 6). Comparison of the morphology of char produced at slow devolatilization in Fig. 5c and the original sample (Fig. 6) suggests that the sample sintered. The structure of char at fast devolatilization heating indicates melting and plastic deformation with ash particles appearing as bright spots. Original coal porosity decreases during devolatilization by either sintering of sample (slow heating rate) or melting of structure (fast heating rate).

The effect of devolatilization heating rate on the structure of coal char can be explained by the thermoplastic properties of coal. At a slow devolatilization heating rate,

Fig. 4 Cumulative pore volumes for **a** original coal and coal chars, **b** original SRM and SRM char samples produced at slow and fast devolatilization heating rates
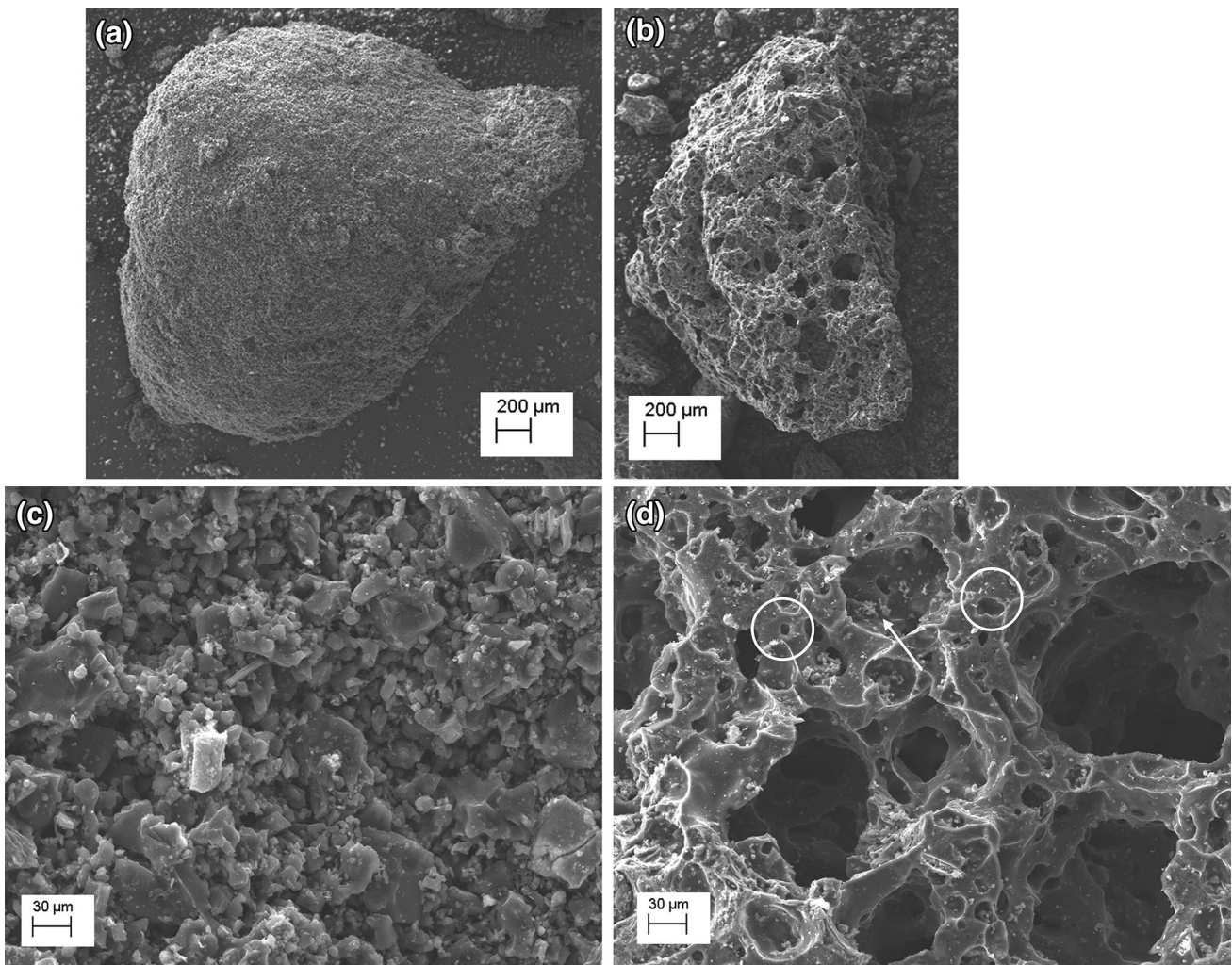

(a)

- sample produced at slow devolatilization
- sample produced at fast devolatilization
- original sample

(b)

- sample produced at slow devolatilization
- sample produced at fast devolatilization
- original sample

Table 5 Effect of devolatilization heating rate on BET Surface area (m^2/g) of SRM char, after crushing to less than 100 µm

Sample	Devolatilization heating rate (K/min)		
	Slow	Medium	Fast
SRM char	17.5	16.9	18.3
Coal char	13.2	13.6	15.5

coal does not show much fluidity, while at a fast devolatilization heating rate, the fluidity is more pronounced. At a high heating rate, coal becomes soft, and pore opening is blocked by the onset of plastic stages. At this stage, volatiles are trapped in the coal and diffuse to form bubbles rather than exiting the coal directly. When a bubble reaches the surface, it releases the volatile matter

[25]. Hence, the coal char produced at a fast devolatilization rate, as shown in Fig. 5d, presents a molten structure and contains larger macropores, while the char produced at a slow devolatilization rate appears as sintered.

SEM images of the original SRM sample (Fig. 7a, b) show diversity in the morphology of this material. Differences in the colors of the observed phases in the back-scattered image (Fig. 7b) suggest the presence of different phases. The effect of devolatilization heating rate on structure of char is less clear for SRM char compared with coal char, as, in both SRM char samples, the compact plastic structure is changed by the release of high amount of volatiles (Fig. 8a, b). The volatile that is released opens some new pores, and the particles consequently develop more macropores compared with the original sample, which is in agreement with the result from mercury porosimetry (Fig. 4b). Investigation of the structure of

Fig. 5 Morphology of the coal char produced at **a**, **c** slow devolatilization; **b**, **d** fast devolatilization, *arrow* in **d** shows the ash particles
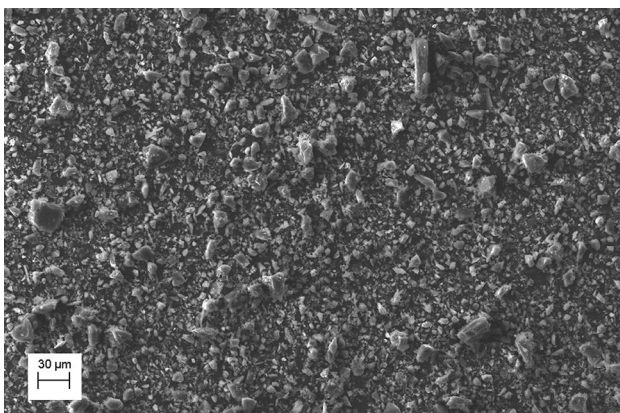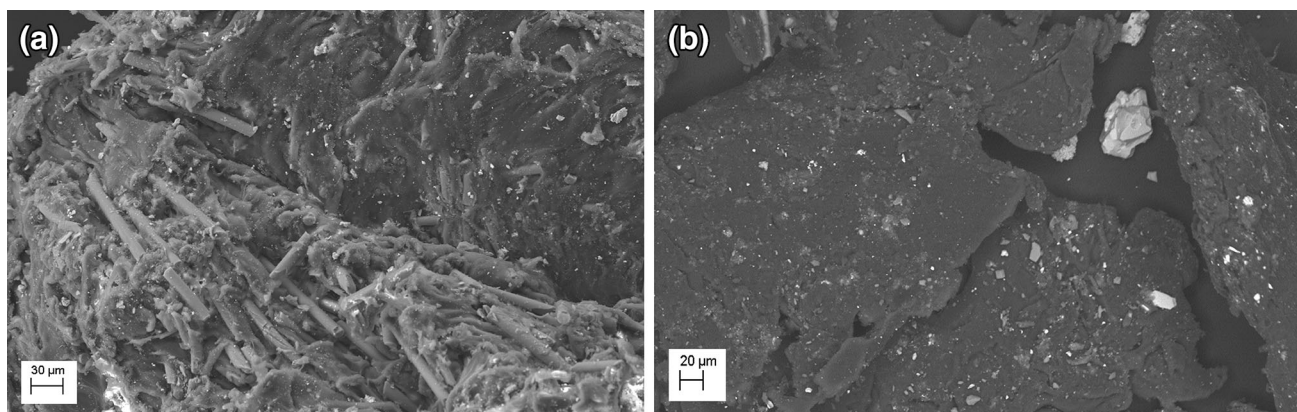

Fig. 6 Morphology of original coal sample

SRM char in Fig. 8 shows that wire-shaped particles still remain after devolatilization, while the rest of structure changed. This result suggests that the mentioned wire-

shaped particles are inorganic parts, which are embedded in the plastic parts.

SRM char produced at fast devolatilization heating rate shows evidence of bubble formation during devolatilization. Figure 9a shows formation of a cenoshpere particle, which is probably formed by the internal pressure caused by release of volatiles inside the formed liquid film. A small hole is observed on top of the particle, which is probably caused by release of volatile. In the other char sample observed in Fig. 9b, the release of volatiles through the melt would lead to an eruption, as can be observed in the SEM image.

Other researchers have also reported formation of a liquid film on the outside layer of high volatiles containing materials [2]. Such a liquid film might be responsible for the formation of some closed pores in the char particles, which could be the reason for decrease in porosity of SRM char produced at a fast devolatilization rate, as observed in mercury porosimetry results.
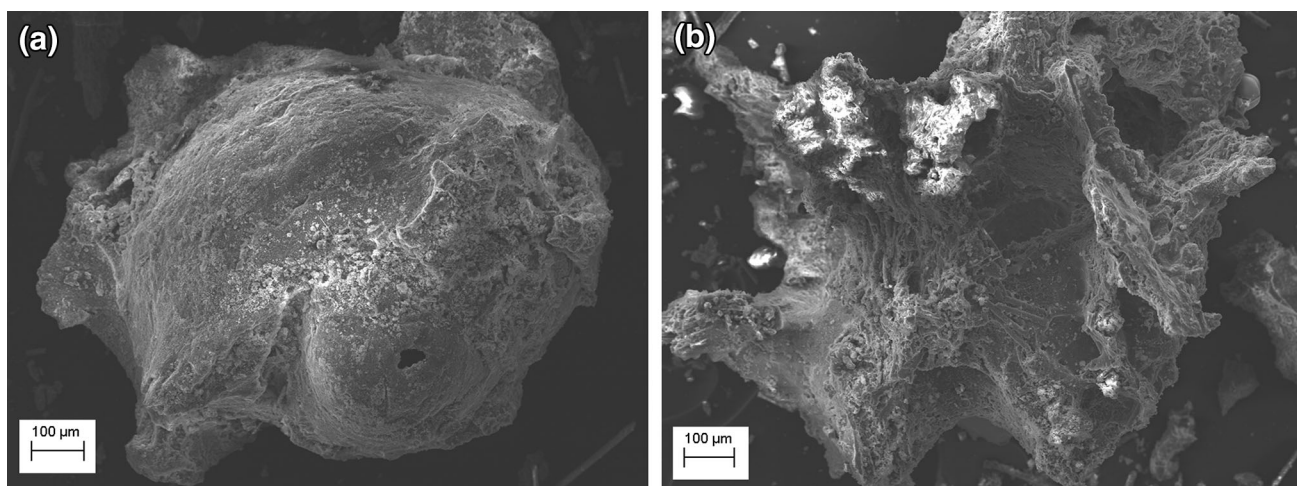
Fig. 7 Morphology of original SRM sample. **a** Secondary electron image. **b** Back-scattered scan
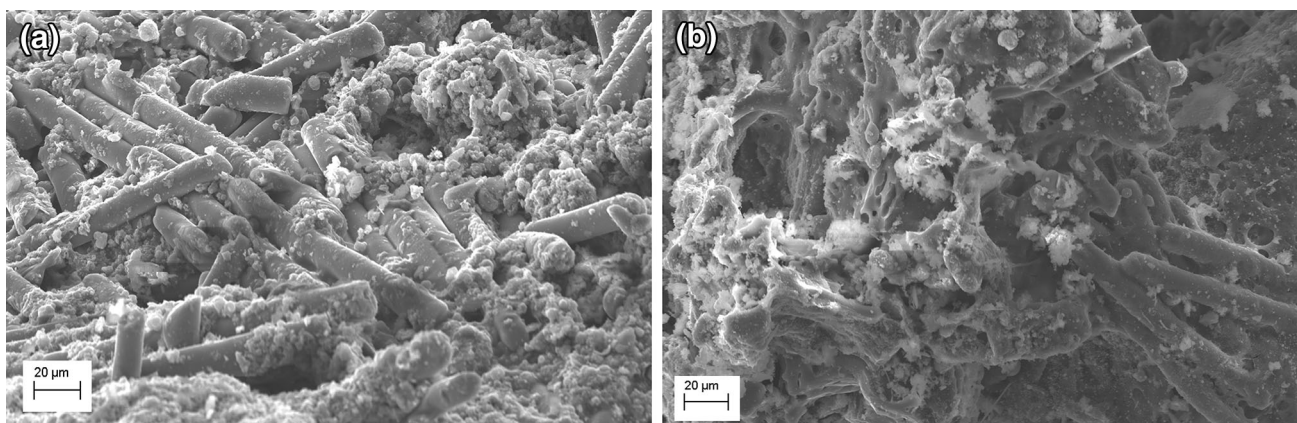
Fig. 8 Morphology of SRM chars. **a** produced at slow devolatilization; and **b** fast devolatilization rate

Fig. 9 SEM images of SRM char produced at fast devolatilization heating rate. **a** Formation of bubble. **b** Erupted bubble

For both SRM and coal char samples, the open and interconnected porous structure in the char sample produced during devolatilization offers an increased number of paths for the gas phase to access carbon sites. A summary of the phenomena occurring during SRM devolatilization is illustrated in Fig. 10. During devolatilization, irrespective of the heating rate, inorganic species do not show any significant changes, while organic

species change completely. The structure of carbon formed by devolatilization of organic parts is affected by the thermal profile that SRM is exposed to.

Gasification Experiments

The effect of temperature on the carbon gasification of char produced at medium devolatilization heating rate was studied, the results are shown in Fig. 11. For both char samples, the time to complete carbon conversion decreased as the gasification temperature increased. At any given temperature and time, the conversion degree of SRM is always higher than that of coal char. Carbon conversion for coal char approaches completion only at temperatures higher than 1273 K, while SRM char reaches complete conversion at temperatures higher than 1173 K.
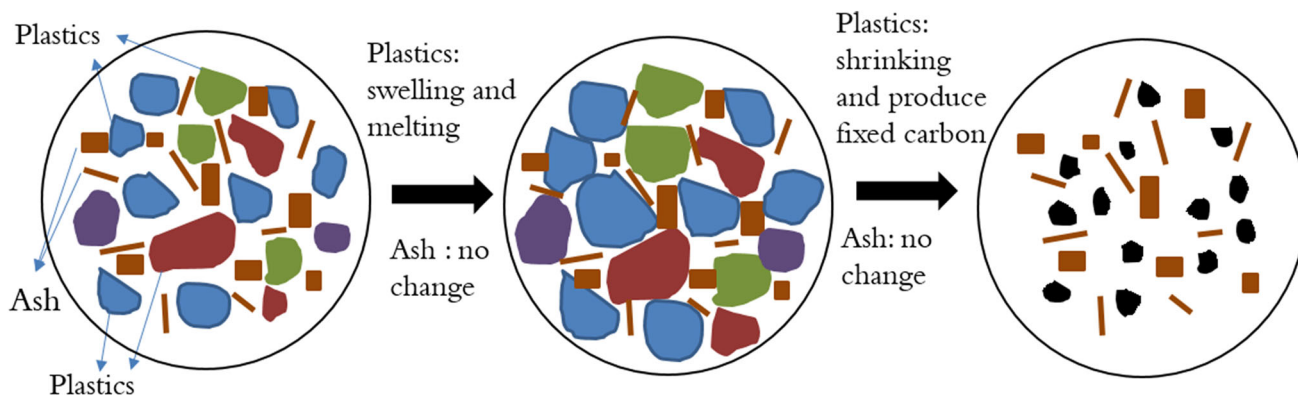
Fig. 10 Schematic illustration of behaviors of the mixture of different plastics as they are heated (inspired from [26])
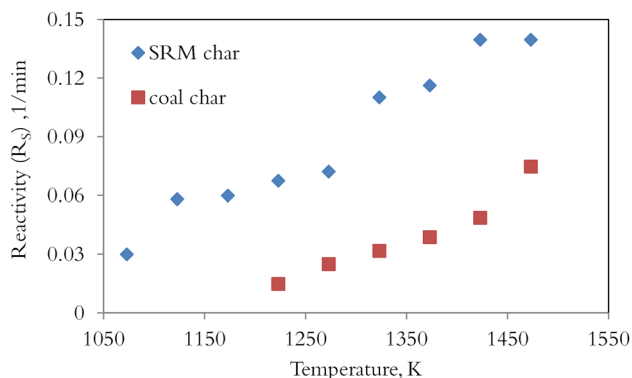

Fig. 11 Carbon conversions at different temperatures for **a** coal char and **b** SRM char during isothermal gasification
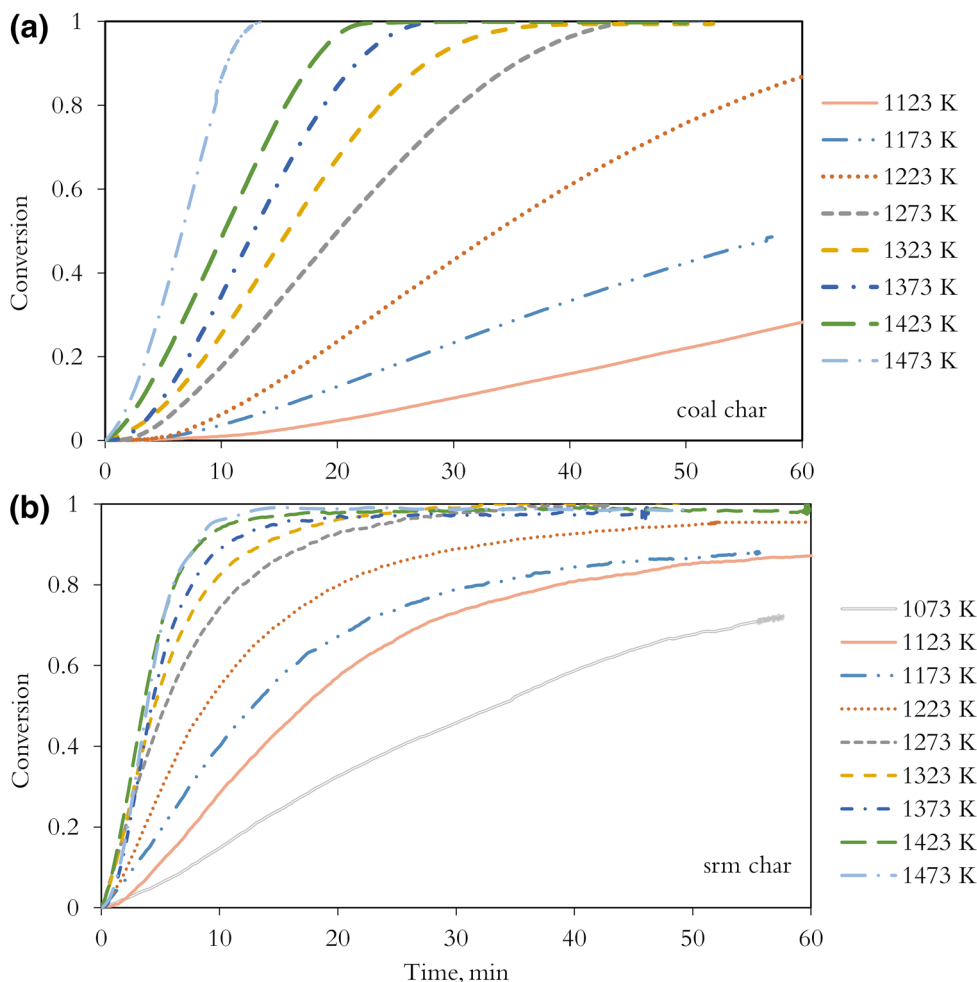
The reactivity index of char gasification is calculated based on Eq. 4, and the result is plotted in Fig. 12. The reactivity index of both char samples increased with the gasification temperature. At each temperature, SRM char shows higher reactivity than coal char.

The gasification kinetic of SRM and coal char during isothermal gasification at the initial stage of reaction is calculated using an Arrhenius plot, which is shown in Fig. 13. The calculated activation energy for coal char is 135.6 kJ/mol, while it is 116.4 kJ/mol for SRM char. At temperatures higher than 1273 K, the activation energy of coal char drops to 74.2 kJ/mol; similarly, the activation energy of SRM char drops to 53.8 kJ/mol at 1273 K. The decrease in the activation energies at these temperatures can be interpreted as a change in the rate-determining mechanism from chemical control to a mixed control, where the reaction occurs under the influence of pore diffusion.

The gasification rate of SRM char was higher than that of coal char; and the estimated activation energy for its gasification was lower than coal char. This difference could be due to different physical properties of material, such as surface area, morphology of char, and the pore distribution, which are known to play a vital role on gasification reactivity [9]. In addition, the ash content, especially alkali and alkaline earth metals (AAEM) and iron, are known to act as catalysts in the gasification reactions. Other inorganic substances such as silica, alumina and phosphates, on the other hand, lower the reactivity of char. Silica has been observed to reduce the reactivity by reacting with potassium to form silicate, blocking the catalytic effect of potassium. Alumina has also been shown to deactivate the catalytic activity of potassium. Potassium phosphate has been observed as inactive in the catalytic carbon gasification. The complicated effects of various ash components are often expressed by alkali index [19, 27]. The alkali index (A value) is calculated by Eq. 6. [28] The alkali

index calculated for coal char is 0.1, while it is 0.4 for SRM char, indicating the higher catalytic effect of SRM char inorganic content, which leads to higher gasification rate and lower activation energy observed for SRM char. Considering utilizing this material in nonferrous metallurgy, after the gasification is completed, the inorganic compound in ash will dissolve in the slag. The process can be designed in such a way that the inorganic compound can be recycled.

$$A = \mathrm{Ash} \times \frac{\mathrm{Fe_2O_3 + Na_2O + K_2O + CaO + MgO}}{\mathrm{Al_2O_3 + SiO_2}} \quad (6)$$

The effects of devolatilization heating rate on the gasification kinetics of char samples are compared using nonisothermal gasification tests. Figures 14 and 15 show the gasification rates versus reciprocals of temperature (Arrhenius plot) during nonisothermal gasification of SRM and coal char.

Table 6 shows the estimated kinetic parameters based on nonisothermal gasification in the temperature range for gasification. Gasification of SRM starts and finishes at lower temperatures, compared with coal char. The activation energies for both SRM char are lower than those of coal char, which is probably due to the mentioned catalytic effect of ash constituents.

The char samples produced at a slow heating rate show lower activation energy compared with char produced at

Fig. 12 Reactivity indices of coal and SRM char measured at different temperatures
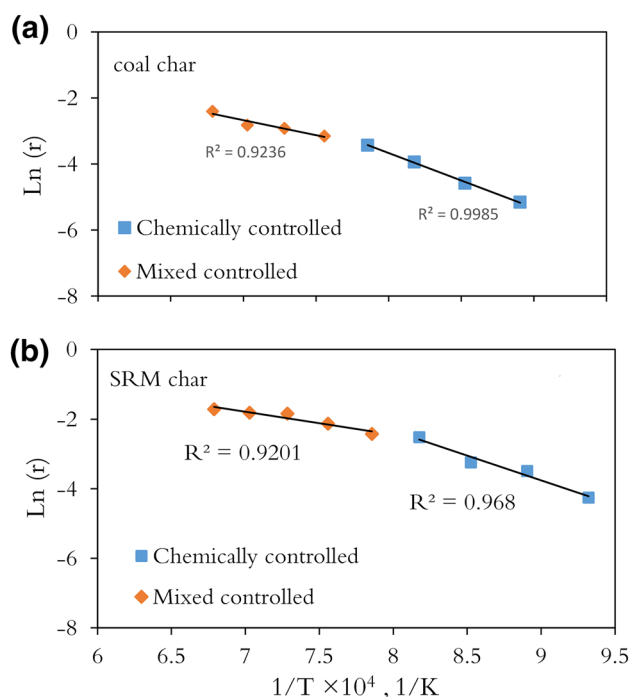
Fig. 13 Arrhenius plots of isothermal gasification at different temperatures. **a** Coal char. **b** SRM char
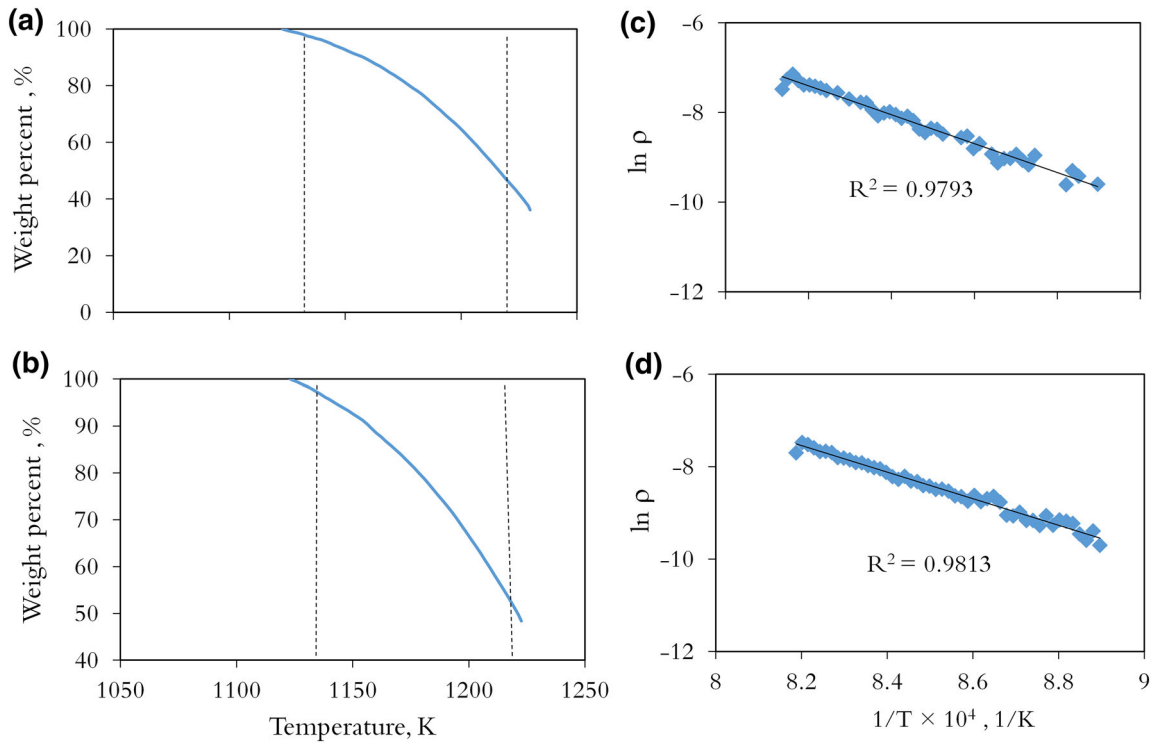
Fig. 14 The weight losses during nonisothermal gasification of char produced at **a** slow devolatilization, **b** fast devolatilization; and Arrhenius plots of **c** at slow, **d** fast devolatilization for coal char samples
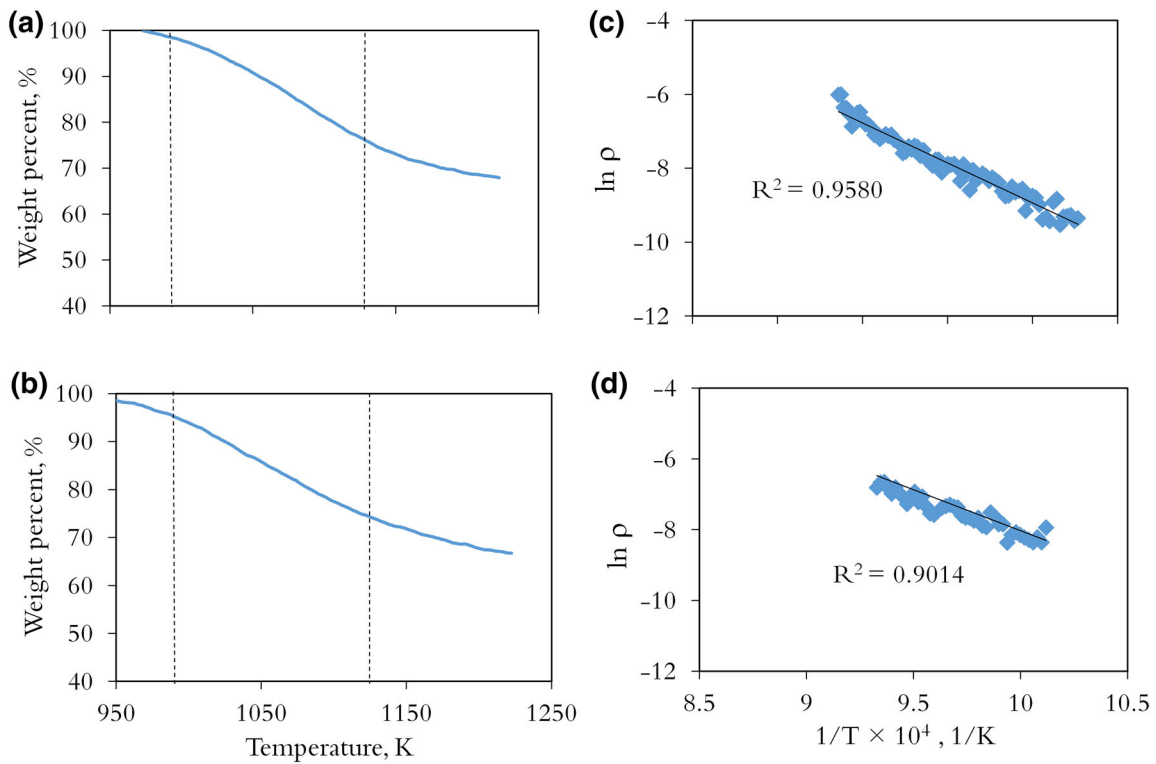
Fig. 15 The weight losses during nonisothermal gasification of char produced: **a** at slow devolatilization, **b** fast devolatilization; and Arrhenius plots: **c** at slow, **d** at fast devolatilizations for SRM char samples

Table 6 Gasification temperatures and kinetic parameters of char samples produced at different heating rates, during nonisothermal gasification experiments

	Devolatilization heating rate	Gasification temperature (K)	Activation energy (kJ/mol)	Preexponential factor (1/s)
Coal char	Slow	1123–1223	281	7.31×10^8
	Fast	1123–1223	238	8.31×10^6
SRM char	Slow	973–1123	179	5.54×10^4
	Fast	973–1123	166	5.41×10^3
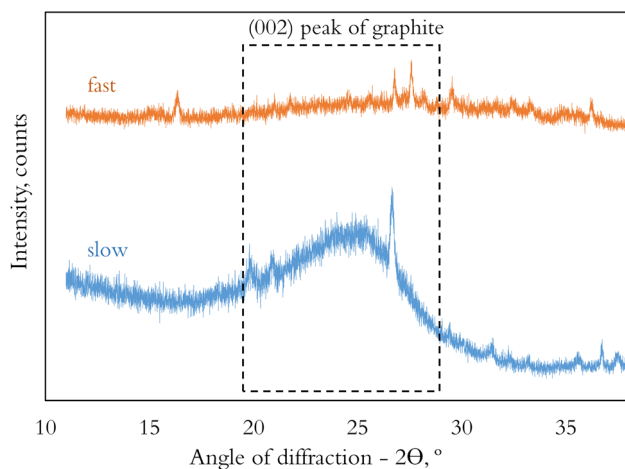
Fig. 16 XRD spectra of SRM chars produced at different heating rates

fast heating rate. In addition, the reactivity of SRM char produced at slow heating rate is lower than char made at a fast heating rate. The structure of carbon in the char is reported to play an important role in char gasification reactivity. It has been reported that char with more ordered crystalline structure has lower ordered gasification reactivity [28]. To examine the effect of devolatilization heating rate on the crystallinity of chars, X-ray diffraction technique was used.

Figure 16 shows the X-ray diffraction spectra of SRM char samples produced at slow and fast devolatilization rate. The position of the peak in the angle region of 27–29°, corresponds to the (002) peak of graphite, which is generally attributed to the stacking of the graphitic basal plans of chars [29]. The disordering of carbon crystalline structure results in the broadening of the (002) diffraction peak: the more disordering of carbon crystalline structure, the wider the diffraction peak of (002) [9]. The char produced at slow devolatilization heating rate shows more order in the structure, indicated by carbon (002) peak accompanied by an overlapping peak of silica, compared with the char produced at fast devolatilization heating rate, which explains the lower reactivity observed for the this char.

Conclusion

- The structure of SRM char and gasification of char are studied to gain a better understanding of its possible application in metallurgical processes. It was found that, although SRM produces a lower amount of char compared with coal char, the SRM char is more reactive than coal char; therefore, the gasification rate is higher.

- Proximate analysis of char shows a higher amount of ash present in SRM char. SRM char contains elements such as copper which has the potential to be extracted during the process; this indicates that utilizing this material in nonferrous metallurgy has the advantage of recycling of the inorganic component.

- SRM char has different physiochemical properties compared with coal char, which would result in different gasification behavior. In addition, the inorganic material present in both char samples has a catalytic effect on gasification rate and activation energy. The isothermal and nonisothermal gasification experiments with char samples show that the gasification of SRM char starts and finishes at a lower temperature compared with coal char. It was also observed that the calculated activation energy is lower for SRM char gasification. Furthermore, the higher gasification rate implies less chance of the unreacted char remaining in the process.

- The effects of devolatilization heating rate on the structure of char samples and their consequent gasification are studied. It was observed that, although the composition of char does not show considerable change, the morphology of char samples differs. Char samples produced at a faster heating rate, which is closer to devolatilization conditions in metallurgical processes, have more disordered crystalline carbon which leads to higher reactivity and, consequently, the gasification rate is higher.

greatly appreciated. This study is within framework of CAMM, Center of Advanced Mining and Metallurgy.

References

1. Ahmed N, Wenzel H, Hansen JB (2014) Characterization of shredder residues generated and deposited in Denmark. Waste Manag 34(7):1279–1288
2. Sahajwalla V, Zaharia M, Kongkarat S, Khanna R, Saha-Chaudhury N, O'Kane P (2009) Recycling plastics as a resource for electric arc furnace (EAF) steelmaking: combustion and structural transformations of metallurgical coke and plastic blends. Energy Fuels 24(1):379–391
3. Babich A, Senk D, Knepper M, Benkert S (2015) Conversion of injected waste plastics in blast furnace. Ironmak Steelmak 43(1):24–30
4. Mirabile D, Pistelli MI, Marchesini M, Falciani R, Chiappelli L (2002) Thermal valorisation of automobile shredder residue: injection in blast furnace. Waste Manag 22(8):841–851
5. Fink JK (1999) Pyrolysis and combustion of polymer wastes in combination with metallurgical processes and the cement industry. J Anal Appl Pyrolysis 51(1–2):239–252
6. Usachev A, Balasanov A, Lekherzak V, Romenets V (2000) Behaviour of coal in smelting reduction installation. Ironmak Steelmak 27(6):426–431
7. Richards G, Brimacombe J (1985) Kinetics of the zinc slag-fuming process: part II. Mathematical model. Metall Trans B 16(3):529–540
8. Cockcroft S, Richards G, Brimacombe J (1988) Mathematical model of lead behaviour in the zinc slag fuming process. Can Metall Q 27(1):27–40
9. Wu H (2015) The CO_2 gasification kinetic study of WEEE plastic char derived from medium temperature pyrolysis. Energy Environ Res 5(1):p82
10. Lin K, Chowdhury S, Wang Z (2010) Catalytic gasification of automotive shredder residues with hydrogen generation. J Power Sources 195(18):6016–6023
11. Brems A, Dewil R, Baeyens J, Zhang R (2013) Gasification of plastic waste as waste-to-energy or waste-to-syngas recovery route. Nat Sci 5:695–704
12. Narobe M, Golob J, Klinar D, Francetic V, Likozar B (2014) Co-gasification of biomass and plastics: pyrolysis kinetics studies, experiments on 100 kW dual fluidized bed pilot plant and development of thermodynamic equilibrium model and balances. Bioresour Technol 162:21–29
13. Zevenhoven R, Karlsson M, Hupa M, Frankenhaeuser M (1997) Combustion and gasification properties of plastics particles. J Air Waste Manage Assoc 47(8):861–870
14. Beamish BB (1994) Proximate analysis of New Zealand and Australian coals by thermogravimetry. N Z J Geol Geophys 37(4):387–392
15. Yao Y, Liu D (2012) Comparison of low-field NMR and mercury intrusion porosimetry in characterizing pore size distributions of coals. Fuel 95:152–158
16. Barranco R, Rojas A, Barraza J, Lester E (2009) A new char combustion kinetic model 1. formulation. Fuel 88(12):2335–2339
17. Liu T, Fang Y, Wang Y (2008) An experimental investigation into the gasification reactivity of chars prepared at high temperatures. Fuel 87(4–5):460–466
18. Wang G, Zhang J, Shao J, Li K, Zuo H (2015) Investigation of non-isothermal and isothermal gasification process of coal char using different kinetic model. Int J Mining Sci Technol 25(1):15–21
19. Lahijani P, Zainal ZA, Mohamed AR (2012) Catalytic effect of iron species on CO_2 gasification reactivity of oil palm shell char. Thermochim Acta 546:24–31
20. Sima-Ella E, Yuan G, Mays T (2005) A simple kinetic analysis to determine the intrinsic reactivity of coal chars. Fuel 84(14–15):1920–1925
21. He R, Sato J, Chen Q, Chen C (2002) Thermogravimetric analysis of char combustion. Combust Sci Technol 174(4):1–18
22. Saxena SC (1990) Devolatilization and combustion characteristics of coal particles. Prog Energy Combust Sci 16(1):55–94
23. Beyler CL, Hirschler MM (2002) Thermal decomposition of polymers. SFPE handbook of fire protection engineering 2. Section 1, Chapter 7, pp 111–131
24. Lowell S, Shields JE, Thomas MA, Thommes M (2012) Characterization of porous solids and powders: surface area, pore size and density, vol 16. Springer, Berlin
25. Yu J, Lucas JA, Wall TF (2007) Formation of the structure of chars during devolatilization of pulverized coal and its thermo-properties: a review. Prog Energy Combust Sci 33(2):135–170
26. Asanuma M, Terada K, Inoguchi T, Takashima N (2013) Development of waste plastics pulverization for blast furnace injection. JFE Tech Rep 19:110
27. Umeki K, Moilanen A, Gómez-Barea A, Konttinen J (2012) A model of biomass char gasification describing the change in catalytic activity of ash. Chem Eng J 207–208:616–624
28. Huo W, Zhou Z, Chen X, Dai Z, Yu G (2014) Study on CO_2 gasification reactivity and physical characteristics of biomass, petroleum coke and coal chars. Bioresour Technol 159:143–149
29. Lu L, Kong C, Sahajwalla V, Harris D (2002) Char structural ordering during pyrolysis and combustion and its influence on char reactivity. Fuel 81(9):1215–1225